Revisiting concrete frost salt scaling

On the role of the frozen salt solution micro-structure

Bahafid, Sara; Hendriks, Max; Jacobsen, Stefan; Geiker, Mette

DOI
10.1016/j.cemconres.2022.106803

Publication date
2022

Document Version
Final published version

Published in
Cement and Concrete Research

Cement and Concrete Research 157 (2022) 106803

Contents lists available at ScienceDirect

Cement and Concrete Research

journal homepage: www.elsevier.com/locate/cemconres

Revisiting concrete frost salt scaling: On the role of the frozen salt solution micro-structure

Sara Bahafid [a,*], Max Hendriks [a,b], Stefan Jacobsen [a], Mette Geiker [a]

[a] NTNU, Department of Structural Engineering, Richard Birkelands vei 1a, 7491 Trondheim, Norway
[b] Faculty of Civil Engineering and Geosciences, Delft Univ. of Technology, 2628 CN, Delft, Netherlands

ARTICLE INFO

Keywords:
Frost salt scaling
Durability
Glue-spall
Freezing and thawing
Modelling

ABSTRACT

We simulate the glue-spall stress due to mechanical interactions between a frozen saline solution (brine-ice composite) and a non-air entrained concrete surface including the impact of the micro-structure of the frozen solution. The presence of brine channels at the ice/concrete interface was found to be a prerequisite to induce stress during freezing and hence for scaling to occur. Pure ice does not result in scaling as it does not have brine channels. Furthermore, the size of the brine channels and their distribution was found determinant for the magnitude of the glue-spall stress in the concrete and the experimentally observed pessimum effect of a medium salt concentration was explained based on the change of the microstructure of the brine-ice composite at different salt concentrations and temperatures. The predicted results are in good agreement with the experimental observations and the few numerical demonstrations related to frost salt scaling in the literature.

1. Introduction

Frost damage is one of the durability issues that faces many Nordic countries and requires expensive repair and maintenance [1–4]. When concrete structures are exposed to freezing and thawing cycles, two types of damage can occur: internal frost damage and surface scaling. The internal damage takes place mostly due to water expansion upon freezing, which generates hydraulic- and crystallization pressure on pore walls and leads to microdamage within the whole concrete body [5,6]. While frost salt scaling (FSS) originates from the interaction between ice and concrete surface in the presence of salt [7–10]. FSS causes superficial progressive damage to the concrete which consists in the removal of small flakes from the material surface. While the internal damage does not require the presence of salt for it to happen, the FSS of concrete is observed when saline solutions are used [11].

FSS has been subject to extensive experimental investigation. However, its modelling has been a difficult task. The difficulty with modelling FSS arises from the lack of a comprehensive theory that accounts for the complex physical, chemical, and mechanical processes behind it. For instance, surface scaling does not occur in the absence of an ice layer on the concrete surface [5,11]. Scaling is observed in the presence of salt in the ice layer while little or no scaling occurs in the case of a pure ice layer on the top of concrete [12,13]. Another major observation related to FSS is that the maximum damage occurs at relatively moderate de-icer concentrations (e.g. 2 to 4% of de-icer by weight), the so-called pessimum concentration [11,14]. In addition, Verbeck and Klieger [11] found that scaling appear independently of the type of solute used for de-icing in their study (i.e. NaCl, $CaCl_2$, Urea and Ethyl alcohol). Moreover, the level of surface scaling increases as the thickness of the ice layer increases [15,16]. Air entrainment of concrete has proven beneficial in improving the concrete resistance to both internal damage and frost salt scaling [4,17,18]. Nevertheless, understanding the mechanisms by which salt generate scaling is still needed.

Recently, Valenza and Scherer [7,13,19] presented a comprehensive theory capable of explaining the FSS and the various intriguing experimental observations related to it. The theory presented by Valenza and Scherer [7,19] is based on an old technique used for glass decorations, called the 'glue-spall' [20]. For instance, during glass manufacturing, an epoxy resin is glued on a sandblasted glass, heated in the oven, and then cooled. As the epoxy resin hardens, it shrinks and cracks into small epoxy-islands. Upon further cooling, each epoxy-island continues to shrink and generates tensile stresses at the boundary of the island that propagate the already existing flaws in the glass and results in small glass particles being removed from the surface [20]. A schematic description of an epoxy-island on a glass substrate is presented in Fig. 1. a, where for convenience the epoxy and glass in the original work of

* Corresponding author.
E-mail address: sara.bahafid@gmail.com (S. Bahafid).

https://doi.org/10.1016/j.cemconres.2022.106803
Received 22 June 2021; Received in revised form 9 March 2022; Accepted 1 April 2022
Available online 14 May 2022

Gulati and Hagy [20] are replaced by ice and concrete. The stresses being generated in the glass (here concrete) and epoxy (here ice) are the result of the large mismatch between their respective thermal expansion coefficients. A schematic description of the horizontal stress distribution in the epoxy (ice, σ_i) and glass (concrete, σ_c and σ_{gs}) is presented in Fig. 1. b. At the concrete interface we distinguish between σ_c the stress in the concrete which is in contact with ice-island, and σ_{gs} (the glue-spall stress) which is the stress in the concrete at the ice-island boundaries. It is seen that while the stress in the concrete along the x direction remains compressive at the centre of the ice-island, it becomes tensile at the boundary of the ice-island and declines to almost zero afterwards [20].

Based on finite element analysis and narrow sealed sandwich theory, Gulati and Hagy [20] proposed an analytical solution for the elastic stresses in ice, σ_i, and concrete, (σ_c, σ_{gs}). The approximation of the extreme values of these stresses (parallel to the x-axis) provided by Gulati and Hagy [20] is given in the following equations, where t_j, E_j, ν_j are respectively the thickness, Young's modulus and Poisson's ratio relative to the material j, where $j \in$ {i = ice, c = concrete}, $\Delta\alpha$ is the mismatch between the thermal expansion coefficients, and ΔT corresponds to the temperature drop of ice and concrete. The equations have been adapted in accordance to the definition of the thickness parameters for the single-sided loading of the concrete as illustrated in Fig. 1.a:

$$\sigma_i = \frac{t_c\left(\frac{E_c}{1-\nu_c}\right)}{\left(\frac{E_c}{E_i}\right)\left(\frac{1-\nu_i}{1-\nu_c}\right)t_c + t_i}\Delta\alpha\Delta T \tag{1}$$

$$\sigma_c = -\sigma_i\frac{t_i}{t_c} \tag{2}$$

$$\sigma_{gs} = \frac{E_c}{1-\nu_c}\left(\Delta\alpha\Delta T - \sigma_i\frac{1-\nu_i}{E_i}\right) \tag{3}$$

Valenza and Scherer [7] argued that the concrete frost salt scaling occurs following a similar process to the glue-spalling. For instance, the mismatch between the thermal properties of the ice and the cementitious material is the cause of the concrete damage [7]. In addition, Valenza and Scherer [7] presented a thermo-visco-elastic analysis of the ice based on the analytical solution provided by Gulati and Hagy [20] where various observations related to FSS were explained. In particular, the damage was related to the fracture behaviour of the brine-ice composite. In fact, the ice having a thermal expansion coefficient five times greater than the concrete, shrinks more upon cooling and is in tension. When the viscoelastic stress in the brine-ice composite exceeds its tensile stress, the brine-ice composite cracks. The cracks in the brine-ice composite propagate into the concrete which result in surface scaling. According to this approach, pure ice does not crack as its tensile stress never exceeds its tensile strength which explains why no scaling occurs in case of frost testing with pure water [7,19]. With increasing salt concentration (up to 3%) the brine-ice composite becomes fragile, as it could be seen from the decline of its mechanical properties presented in Table 1 (values corresponding to T = −20 °C). The decrease of the tensile strength of the brine-ice composite as the salt concentration rises makes it more likely to fracture. At higher salt concentration (beyond 3%), the highly porous brine-ice composite does not have sufficient strength to generate enough stresses on the concrete surface and thus does not result in concrete scaling [7,19].

Çopuroğlu and Schlangen [15] investigated the frost salt scaling through both experiments on concrete and modelling of the glue-spall with a lattice model. Their simulations were capable of reproducing

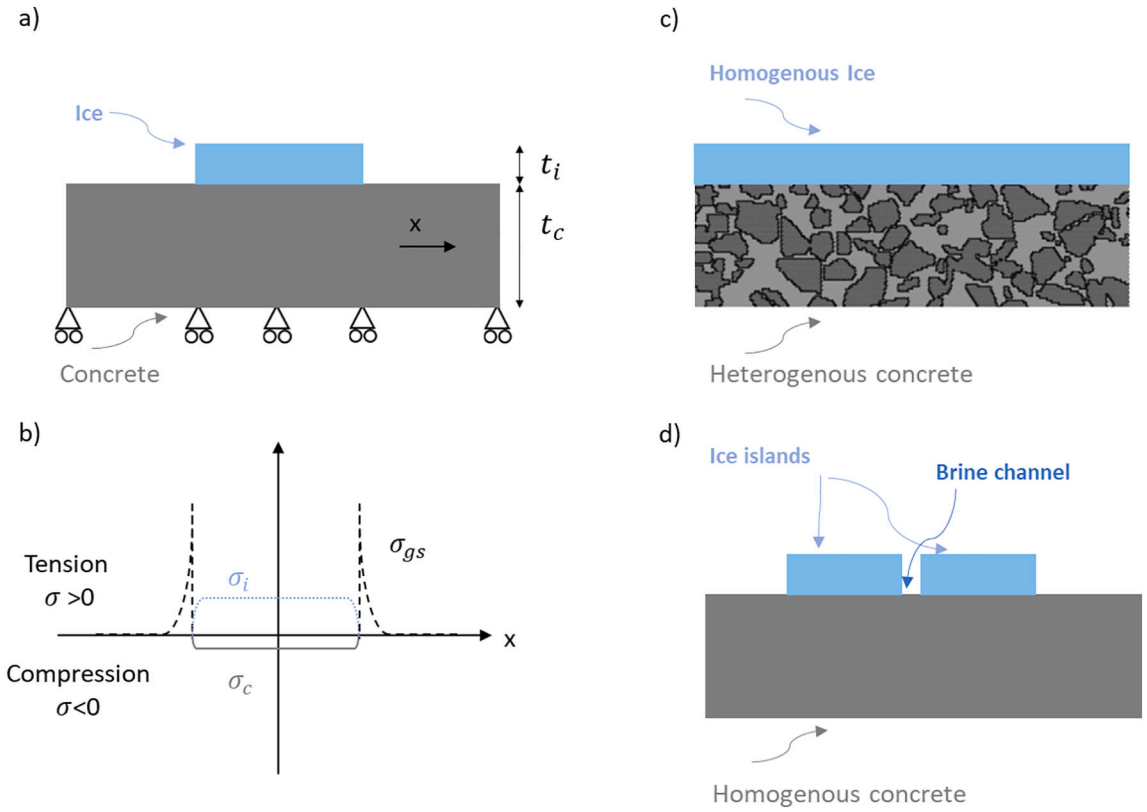

Fig. 1. (a) Description of the seal geometry used for modelling the glue spall mechanisms in the original paper by Gulati et Hagy [20]. The figure has been modified for convenience, where the epoxy is replaced by the ice and the glass by the concrete and where the two-sided loading of the glass is replaced by a single-sided loading of the concrete. (b) A schematic description of the stress distribution of ice and concrete, based on Gulati and Hagy [20]. (c) Description of the geometry used for modelling the FSS in Çopuroğlu and Schlangen [15] with homogenous properties of the brine-ice. (d) The geometry adopted in this study, where the brine-ice composite is nonhomogeneous and composed of isolated ice island separated by brine channels.

Table 1
Mechanical properties of brine-ice composite for different salt concentrations at T = −20 °C. The values are derived from relevant equations relating the Young's modulus and tensile strength to the brine volume fraction φ_b. The Young's modulus was estimated from the equation provided by Vaudrey [21] (E(GPa) = $10\,exp\left(-7.1\sqrt{\varphi_b}\right)$). The ice flexural strength was estimated from the following equation $\sigma_{T-ice} = 1.76\,exp\left(-5.88\sqrt{\varphi_b}\right)$ provided by Timco and O'Brien [22].

Salt concentration (%)	Pure ice	1%	3%	5%
Young's modulus (GPa)	10	2.23	0.74	0.34
Flexural strength (MPa)	1.80	0.50	0.21	0.11

some of the important features of FSS such as the existence of a pessimum salt concentration and the increase of salt scaling with increasing ice thickness. Table 2 recapitulates the literature work discussed here together with the assumptions relative to these studies. It can be seen that the different studies presented in Table 2 assume homogenous properties of ice. In what follows a demonstration of the limitation of this assumption is given. For instance, in modelling of FSS by Çopuroğlu and Schlangen [15] and Valenza and Scherer [7], the ice was considered as a homogenous slab (see Fig. 1.c) with its mechanical properties decreasing with increasing salt concentration (see Table 1). Let us examine the glue-spall stress in the concrete, just outside the ice-island, for two different scenarios: pure ice on the top of concrete and NaCl 3%-ice on the top of concrete, and estimate this stress based on Eq. (3). The predicted glue-spall stress (the stress in the concrete at the ice-island boundaries), for these two cases is presented in Fig. 2, where the corresponding material properties used for ice, 3%-NaCl ice and concrete are recapitulated in Table 3. It is seen from Fig. 2 that the glue-spall stress is higher in the case of pure ice, owing to the higher mechanical properties of the pure ice. Therefore, pure ice would be expected to cause a higher damage to concrete than a brine-ice, which is contradicting to the well-established observations related to FSS. Consequently, a modelling approach based on the glue-spall theory while considering the homogenized mechanical properties of the brine-ice composite is incompatible with experimental observations.

Similarly, the approach proposed by Valenza and Scherer [7] based on the fracture behaviour of brine-ice, seems to be limited when trying to explain the increasing concrete scaling with increasing ice layer thickness. For instance, the stress in the brine-ice is inversely proportional to the brine-ice thickness as can be seen from Eq. (1). Correspondingly, the stress in the brine-ice composite decreases as its thickness increases. At a given temperature, the stress will exceed the tensile strength of the thinner brine-ice composite, while it is still below the tensile strength in the case of a thicker brine-ice composite. According to the approach presented by Valenza and Scherer [7,19], the thinner brine-ice composite will then fail and will be more likely to crack and propagate cracks in concrete. However, experiments show that concrete scaling increases with the increase of the ice layer thickness [15,16,42]. An explanation of the increased concrete salt scaling when the ice thickness increases seems groundless if we only consider the fracture behaviour of homogenous ice as presented by Valenza and Scherer [7].

Table 2
Compilation of literature work analysed and discussed in this study and the assumptions related to the different studies.

	Material	Modelling and assumptions
Gulati and Hagy [20]	Homogenous epoxy and glass (geometry as Fig. 1.a)	Elastic stresses in epoxy and glass
Valenza and Scherer [7]	Homogenous ice	Modelling viscoelastic stresses in the ice
Çopuroğlu and Schlangen [15]	Homogeneous ice and heterogeneous concrete (Fig. 1.c)	Elastic stresses in ice and concrete, crack development in ice and concrete
This study	Heterogeneous ice (brine-ice composite) and homogenous concrete (Fig. 1.d)	Viscoelastic stresses in brine-ice composite and concrete

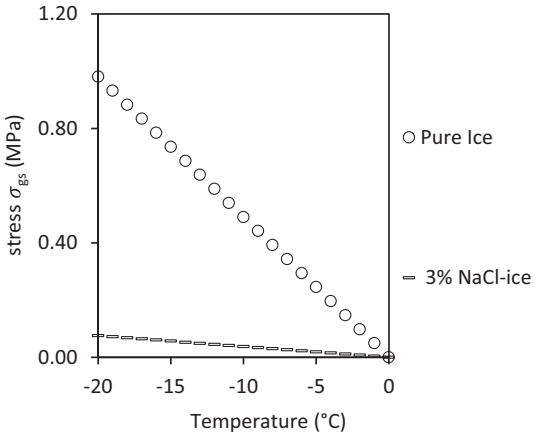

Fig. 2. Evaluation of the stresses σ_{gs} based on the analytical estimation of stress at the concrete interface close to ice boundaries provided by Gulati and Hagy [20]. The typical values of thermal and mechanical properties of ice, 3% NaCl-ice and concrete presented in Table 3 are used in the calculation.

Table 3
Typical values of thermal and mechanical properties of ice and concrete used in FSS experiments (adapted from Valenza and Scherer [6]).

Material	Pure ice	3% NaCl-ice	Non-air entrained cement paste
Young's modulus, E (GPa)	10	0.74	25
Poisson's ratio, ν	0.33	0.33	0.2
thermal expansion coefficient, α ($°C^{-1}$)	5.1×10^{-5}	5.1×10^{-5}	1.0×10^{-5}
Thickness (mm)	3	3	36

It is clear from the above presented review that considering the homogenous behaviour of the brine-ice is inconsistent with some experimental observations. The glue-spall theory supports that the presence of gaps is a pre-requisite for the build-up of tensile stresses at the concrete surface. Indeed, during freezing of a salt solution on a concrete material, the solute ions are ejected outside the ice and contained in the brine pockets and the brine channels [23,24]. Various ice-islands form on the surface with brine channels between them. Upon lowering the temperature, the ice-islands grow together to form a porous material, depending on the salt concentration. When the ice-islands are isolated, stresses at the boundaries of these ice-islands will generate tensile stresses at the concrete surface. However, in the previous studies [7,15,20], the effect of the film (ice in this case) microstructure was not investigated. For instance, how the synergy created between different isolated islands covering the substrate (i.e. Fig. 1.d) would affect the stress distribution on the substrate, was not discussed. Furthermore, the saline ice layer is a dynamic porous medium where the ice fraction and correspondingly the brine fraction (brine filled porosity) evolve with the temperature and the bulk salinity of the ice [25]. Similarly, the brine-pockets or pores vary in size, distribution, and degree of connectivity [24,26]. These changes related to the ice microstructure are likely very important in the build-up of stresses at the concrete surface, which leads us naturally to inspect its effects on the stress build-up at the ice concrete interface. For instance, how would the brine channel size and the island-width influence the magnitude of stresses that build-up at the surface of concrete during a freeze-thawing cycle need to be investigated.

The aim of this paper is to extend the glue-spall theory and provide further insights on the parameters that have a critical influence on the FSS. The model is intended to address the mechanical surface interactions between the brine-ice layer and the concrete substrate. The

present paper has the following objectives. First, it presents a numerical simulation of the glue-spall theory to simulate the elastic stresses in ice and concrete as a function of temperature. Second, it extends the glue-spall theory to account for the effect of ice microstructure on the magnitude of simulated stress (as recapitulated in Fig. 1.d), where the effect of the ice-island width, thickness and the gap between two-neighbouring-islands is explored. Finally, it presents explanations for the different mechanisms related to FSS based on the glue-spall and the ice microstructure.

2. Modelling aspects

2.1. Geometry and boundary conditions

Numerical simulation of thermal stresses generated due to the thermal mismatch between ice and concrete during a temperature cycle was simulated using COMSOL finite element analysis code. Different geometries corresponding to a bi-layer material ice (or ice-islands) covering a concrete substrate were simulated. In 2D plane stress analyses, the concrete specimen had a width of 65 mm and a thickness of 20 mm. The ice-islands width and thickness, as well as the spacing between the two islands will change throughout the paper, as the effects of the geometrical aspects related to ice were of interest in this study. First the assumptions linked to the glue-spall theory were investigated. Secondly, in an attempt to explain the different observations related to salt scaling, based on the glue-spall theory, the effect of the ice geometry and its distribution along the concrete surface were investigated. Three parameters were studied: the width of the ice-island, the distance between two neighbouring ice-islands and finally the thickness of the ice-island. Various numerical simulations corresponding to two separate pure ice-islands on the top of concrete surface (as in Fig. 3.c), were performed while only varying the parameter of interest and keeping the other parameters constant. The four following cases were simulated:

i.1 A comparison of the effect of the ice homogeneity on the stress distribution was conducted. Numerical simulations were performed for two geometries (case 1),

- where a homogenous ice layer is covering the entire concrete surface Fig. 3.a (homogenous ice).
- where a homogenous ice-island is partly covering the concrete surface Fig. 3.b. This configuration is intended to represent heterogonous ice in the sense that the ice has brine channels, represented by boundaries with the concrete.

i.2 The effect of the island width is investigated by varying the width w_i of the two ice-islands from 5 mm to 30 mm, while the gap d_i between these two islands and their thicknesses t_i were kept at 1 mm and 2 mm respectively (case 2, Fig. 3.c).

i.3 The effect of the gap size between the two-ice-islands was examined by keeping the ice-islands width to 25 mm and thickness to 2 mm, while the gap between the two neighbouring-islands was varied from 0.1 mm up to 5 mm (case 3, Fig. 3.c).

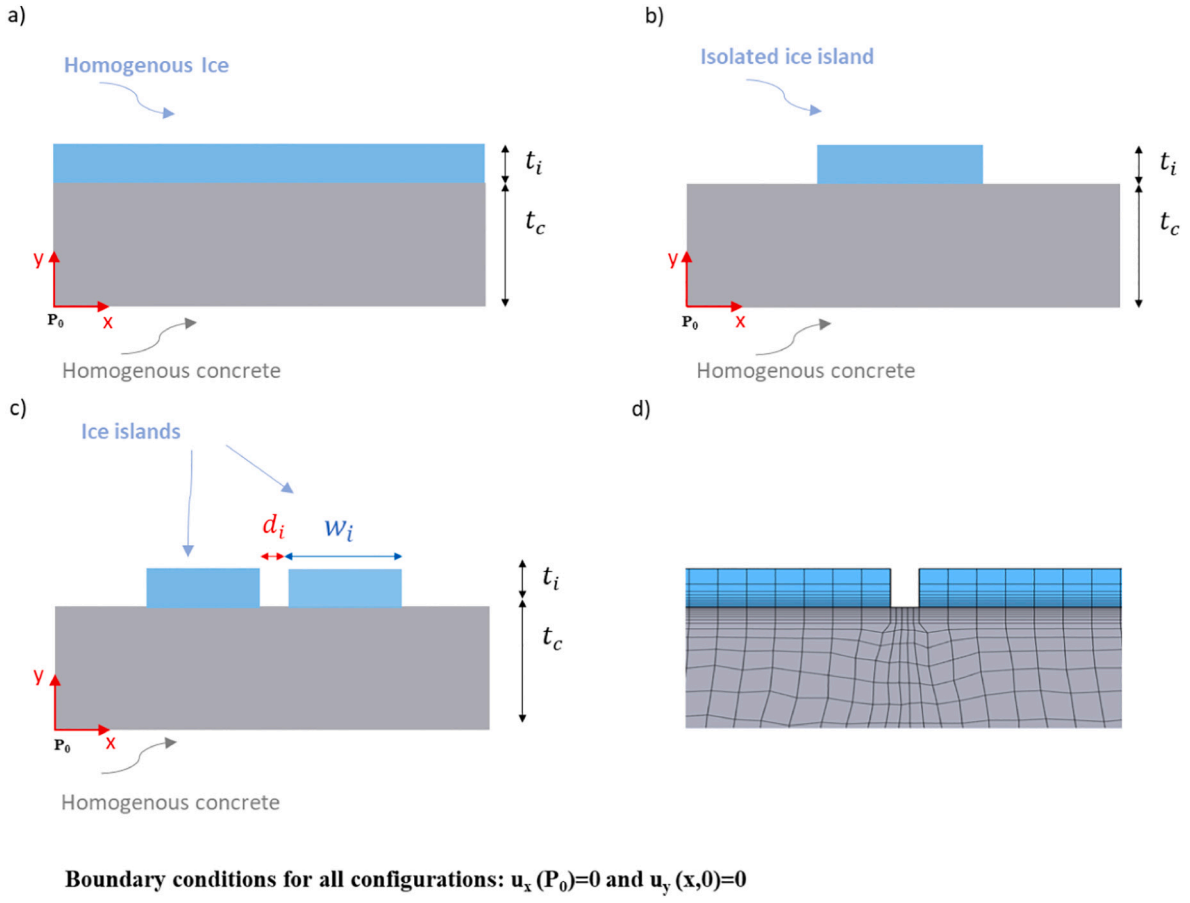

Fig. 3. Geometry and boundary conditions used in the numerical analysis: (a) a homogenous ice layer covering a concrete substrate. (b) An isolated ice-island partially covering the concrete substrate. (c) Two ice-islands are placed symmetrically on the top of a concrete substrate with a gap separating them. The concrete had a width of 65 mm and a thickness of 20 mm. The widths and thicknesses and gap sizes of ice-island vary in simulations and are recapitulated in appropriate sections of the paper. The movement are pinned in the corner (0,0), while the displacement along the y-axis are prevented at the bottom of the substrate (y = 0). (d) A detail of the finite element model with a refined mesh close to the expected glue-spall peak stresses.

i.4 The thickness of the ice-island was explored, where the thickness of the two ice-islands covering the concrete was varied from 1 mm to 10 mm, while keeping the ice width at 25 mm and the gap size at 1 mm (case 4, Fig. 3.c).

For all simulated cases a perfect bond between the ice and the concrete substrate is assumed. Mapped meshing with quadrilateral shaped elements was used. The element size was minimised near the film-substrate surface (Fig. 3.d), as this area is very prone to stress concentration. A fine mesh was also introduced at the gap between two neighbouring ice-islands. For the different simulations 5 elements were distributed over the gap between the two ice-islands. Movements were restricted in all directions at the bottom left corner (x = 0, y = 0), while the displacement along the y-axis were prevented at the bottom of the substrate (y = 0) (Fig. 3).

The applied thermal loading is described in Fig. 4, where the reference temperature is set to $T = 20$ °C. The considered temperature variation is comparable to temperature cycles usually applied when testing concrete for frost salt scaling [16]. During the simulation of the freeze-thawing cycle, the ice phase is considered active only when the temperature drops below $T = 0$ °C.

2.2. Solid mechanics background

The model presented hereafter is intended to describe the effect of a temperature change on a bi-layer material (ice/concrete). The mechanical behaviour of the bi-layer material is described within the framework of thermo-elasticity assuming that both concrete and pure ice are isotropic. Considering the infinitesimal theory of elasticity, the strain is related to displacements u via the following equation where ε is the symmetric strain tensor:

$$\varepsilon = \frac{1}{2}\left(\nabla_u + \nabla_u^T\right) \tag{4}$$

The equilibrium equations can be written, when neglecting the inertial terms as follows, where σ is the stress tensor and F_V refers to the body forces:

$$\nabla_\sigma + F_V = 0 \tag{5}$$

The stresses are related to the elastic strains via the Hooke's law as follows, $C(E, v)$ being the 4th order elasticity tensor for isotropic material which is a function of the Young's modulus and the Poisson's ratio of a material:

$$\sigma = C(E, v) : (\varepsilon - \varepsilon_{th}) \tag{6}$$

The thermal strains are related to the temperature change and the thermal expansion coefficients of the given material via the following equation:

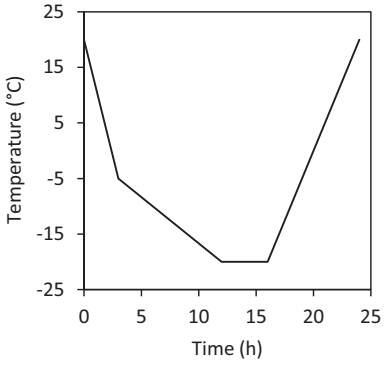

Fig. 4. The temperature cycle applied during simulations for generating frost scaling damage. This cycle corresponds to typical cycles applied during freeze-thawing of concrete.

$$\varepsilon_{ij(T)} = -\alpha(T - T_0)\delta_{ij} \tag{7}$$

δ_{ij} being the components of the unit tensor I and T_0 is the strain reference temperature.

2.3. Heat transfer background

The heat transfer in continuum medium is governed by the following equation assuming only conduction and uncoupled thermo-elasticity:

$$\rho C_p \frac{DT}{Dt} - \lambda \nabla T = 0 \tag{8}$$

ρ being the density, C_p is the specific heat capacity, λ the thermal conductivity and ∇T is the temperature gradient.

2.4. Creep in the ice

Ice exhibits rapid creep which leads to rapid stress relaxation within the ice. In addition to the thermo-elastic description provided above, the creep in the ice is accounted for. The temperature-dependent creep behaviour of the ice is well described in the literature [27–29]. It was shown that over a large temperature range the creep behaviour can be described by a single equation [27], which is a modified version of the creep power-law equation [30], where A is an empirical constant, Q is the energy activation, R is the universal gas constant and T is the temperature:

$$\dot{\varepsilon}_{Cr} = A\ sinh(\beta\sigma_e)^n e^{-\frac{Q}{RT}} \tag{9}$$

The empirical constants were calibrated on experiments and depend on the temperature range [27]. The thermo-mechanical properties of ice and concrete used for the modelling and the empirical constants used in the creep law equation are, reported respectively in Tables 4 and 5.

3. Results

3.1. Validation of the glue-spall theory: application to the bilayer material ice/concrete-case 1

The results corresponding to the geometries presented in Fig. 3.a and b are presented in Fig. 5, where the stresses at the uppermost surface of concrete (y = 20 mm) parallel to the x-axis (σ_{xx}), and the parallel to the y-axis (σ_{yy}) and the shear stress (σ_{xy}) are presented, along the x-axis. The stresses correspond to $t = 12$ h, where the temperature reaches −20 °C for the first time, as it can be seen from the temperature cycle in Fig. 4. It is worth noting that the stresses are higher at t = 12 h, as although the temperature is kept constant at −20 °C for a couple of hours, the creep in the ice results in important stress relaxation and thus decreases the stress at the concrete interface. It can be clearly seen that the stresses parallel to the x-axis (σ_{xx}) at the concrete surface are compressive (i.e. <zero) at the region of contact between the concrete and the continuous ice layer or ice-island. When we approach the boundary of the ice-island, the

Table 4
Input parameters used in the numerical modelling.

Property	Notation	Value		Unit
		Pure ice	Concrete, non-air entrained	
Young's modulus	E	10 [7]	≈24 [31,32]	GPa
Poisson's ratio	ν	0.33 [7]	0.2 [7]	–
Thermal expansion	α	5.1×10^{-5} [7]	10×10^{-6} [7,33]	1/K
Thermal conductivity	λ	2.16 [33,34]	≈2.6 [35]	W/m·K
Heat capacity	C_p	2110 [33,34]	1100 [36]	J/kg·K
Density	ρ	917 [33,34]	2130 [36]	kg·m^2

Table 5
Creep law parameters for undamaged isotropic polycrystalline ice adapted from Barnes et al. [27].

Creep law empirical parameters	−2 to −8 °C	−8 to −14 °C	−14 to −22 °C	Unit
A	4.6×10^{18}	3.14×10^{10}	1.88×10^{10}	
Q	120	78.1	78.1	kJ/mol
β	0.279	0.254	0.282	MPa^{-1}
n	3.14	3.08	2.92	–

stress (σ_{xx}) becomes tensile (i.e. >zero), with its peak value being at the edges of the ice and then declines rapidly as we move away from the ice-island boundary.

The stresses (σ_{xx}) along the x-axis in the case of a continuous ice layer stay compressive over the whole concrete surface. Furthermore, the stresses parallel to the y-axis (σ_{yy}) and the shear stress (σ_{xy}) are negligible at the region where ice and concrete are in contact and increase at the proximity of the ice boundary to become tensile and drop thereafter. Similarly, (σ_{p1}) the first principal stress, is only non-negligible at the boundaries of the ice. It is worth mentioning that the peak values of the stresses at the edge are greatly dependent on the mesh and will increase upon mesh refinement. The stress distribution in concrete and at the ice concrete boundaries are in line with the glue-spall analysis provided by Gulati and Hagy [20], where it is shown that the tensile stresses build-up at the boundaries of the epoxy. Results in Fig. 5 confirm that the presence of boundaries between ice and concrete is essential for the build-up of tensile stresses at the concrete surface and thus for the scaling to occur.

3.2. Implication of the ice geometry on frost salt scaling

3.2.1. Effect of ice-island width on the stress distribution at the concrete interface (case 2)

The stress parallel to the x-axis (σ_{xx}) corresponding to case 2 where the two-neighbouring ice-islands have varying widths w_i, while the gap $d_i = 1$ mm and the thickness $t_i = 2$ mm is presented along the x-axis in Fig. 6. It is clearly seen that the smallest ice-island of 5 mm width results in lower tensile stress at the gap between the two islands on the concrete surface. Upon increasing the island width from 5 mm to 15 mm the stress at the gap increased. Further increasing of the ice-island width beyond 15 mm did not result in an increase of the stress level. It is worth noting that the tensile stress builds up a few mm before reaching the ice boundary and it reaches its highest value nearby the edge. This is suggesting that depending on the tensile strength distribution of the concrete surface, the particle being removed from the concrete surface might cover both the gap region and the ice-covered region nearby the gap. Fig. 7 shows the distribution of stress parallel to the x-axis (σ_{xx}) at the center of the bi-layer material, where it can be confirmed that the scalloped particle can be expected at the gap and the small region nearby.

3.2.2. Influence of the gap size between neighbouring ice-islands on the stress distribution at the concrete interface (case 3)

The distribution of stress parallel to the x-axis (σ_{xx}) along the x-axis corresponding to case 3, where the gap d_i between the neighbouring ice-

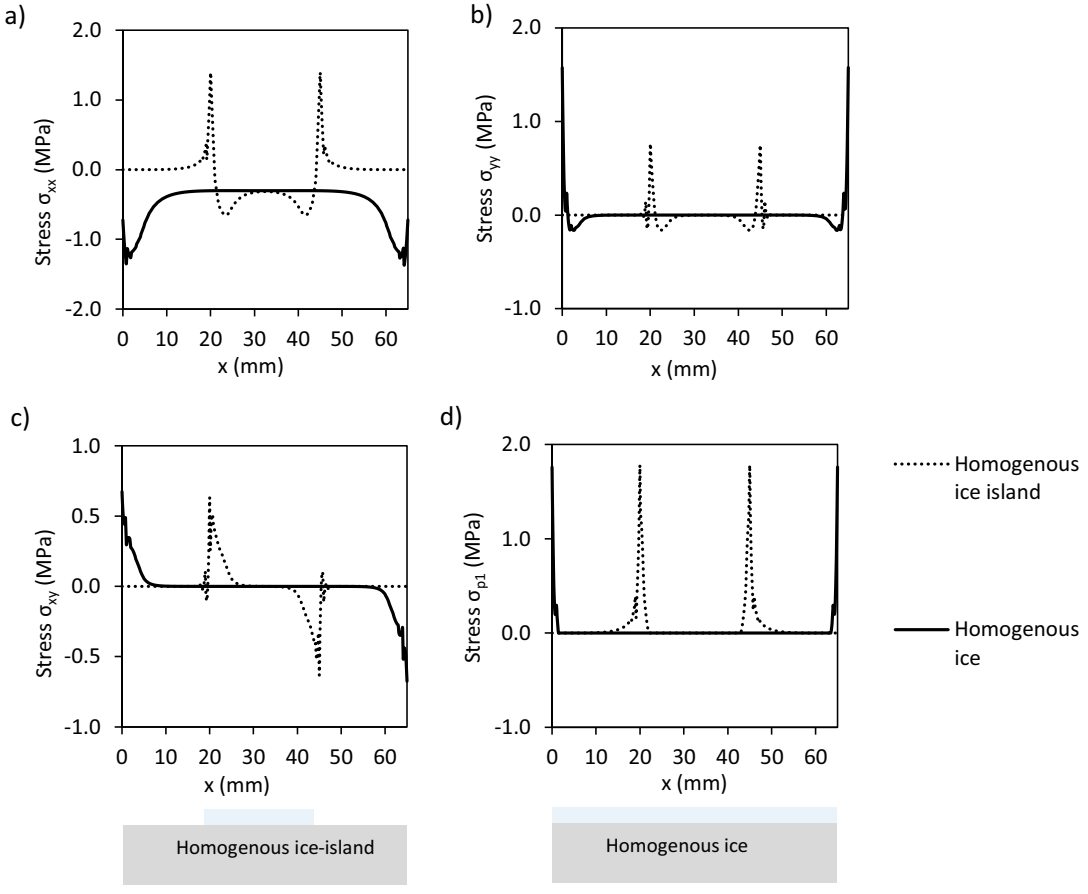

Fig. 5. Overview of the stress distribution at the uppermost surface of concrete (y = 20 mm) for two different ice geometries (a continuous ice layer (65 mm width and 2 mm thickness, Fig. 3.a) covering the entire concrete surface and an ice-island (25 mm width and 2 mm thickness, Fig. 3.b) covering a part of the concrete surface). The results correspond to t = 12 h and T = −20 °C. σ_{xx}, σ_{yy}, σ_{xy} are respectively the stress parallel to the x-axis, y-axis, and shear stress. σ_{p1} is the 1st principal stress.

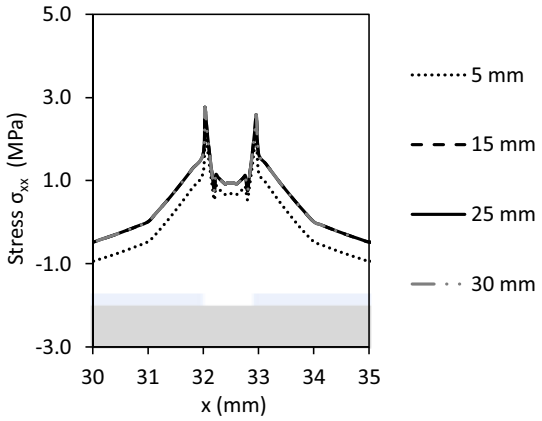

Fig. 6. Results of the simulation corresponding to two ice-islands on a concrete substrate, where the island width was varied from 5 mm to 30 mm, while the gap between these two islands and their thicknesses are kept at 1 mm and 2 mm respectively (results corresponding to case 2). The results correspond to the uppermost surface of concrete (y = 20 mm), t = 12 h and T = −20 °C.

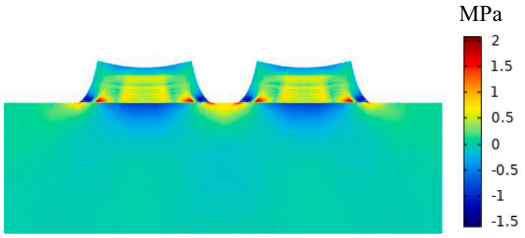

Fig. 7. Stress distribution corresponding to two-neighbouring islands (5 mm in width and 2 mm of thickness) placed on the top of a concrete surface. The gap between the two island is of 1 mm, the results corresponds to t = 12 h and T = −20 °C.

islands was varied while keeping the islands-width and thicknesses fixed to respectively w_i = 25 mm and t_i = 2 mm, is presented in Fig. 8. The effect of the gap on the stress distribution is obvious. It is clear that reducing the gap size between the two ice-islands increases the stress at the level of the gap between the ice-islands. For instance, the stress at the center of the gap increases from 0.22 MPa at 5 mm to 3.7 MPa at 0.1 mm. Further decreasing of the gap between ice-islands will lead to further

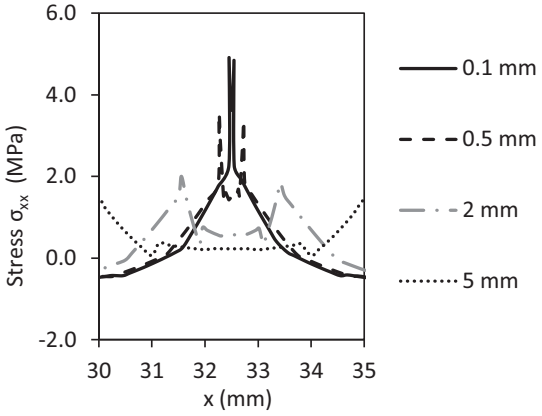

Fig. 8. Results of the simulation corresponding to the case 3 where the two-ice-islands have a width of 25 mm and thickness of 2 mm. The gap between the neighbouring islands was varied from 0.1 mm up to 5 mm. The results corresponds to the uppermost surface of concrete (y = 20 mm), t = 12 h and T = −20 °C.

increase of the stress level. It seems that reducing the gap size between two neighbouring ice-islands leads to an increase of the stress at the gap as a result of the interference between the two ice-islands. Fig. 10 shows the stress distribution parallel to the x-axis (σ_{xx}) for both concrete and ice bi-layer material. Indeed, the maximum of tensile stress occurs at the gap level. It is again clear that the size of the gap influences the size of the zone where the tensile stress builds up (the damage zone), with a narrow gap resulting in higher stress and smaller damaged zone compared to a wide gap.

In Fig. 9 the stresses at the center of the gap between the two neighbouring-ice-islands are presented, for different gap sizes, when the material is subjected to the temperature cycle presented in Fig. 4. It is clear that upon lowering the temperature, the tensile stresses generated at the gap level increase. When the temperature reached T = −20 °C, at t = 12 h, the stresses started decreasing slowly while the temperature was held constant. This is attributed to the progressive stress relaxation in the ice. One can also note a change in the slope of stress variation with temperature where two different slopes are identified. The change in stress build-up rate is the combined action of the temperature dependant behaviour of the ice-creep and the change in the freezing rate during the freezing process. Furthermore, when the temperature is increased, the stresses become compressive at the gap level, which is an effect of the creep in the ice. During the thawing, tensile stress develops underneath the ice as well (not presented here). However, these tensile stresses remain lower compared the tensile stresses observed in the gap during the freezing process. This would suggest most of the scaling would occur during the freezing of the concrete.

3.2.3. Effect of the ice thickness on the stress distribution at the concrete interface (case 4)

The stress parallel to the x-axis (σ_{xx}) corresponding to the 4th case where the thickness t_i of the ice-islands was varied from 1 mm to 10 mm while keeping the islands-width fixed to (25 mm) and the gap between the ice-islands at 1 mm, is presented along the x-axis in Fig. 11. Evidently, the thickness of the ice has a direct influence on the magnitude of stresses at the gap level. It is apparent that increasing the thickness of the ice leads to increasing stress at the level of the gap between the ice-islands, as expected. For instance, the stress at the center of the gap rises from 0.68 MPa for 1 mm thick ice to 1.14 MPa for a 10 mm thick ice. For instance, the thinner the ice, the less it is capable of deforming the concrete, and therefore results in lower stresses at the surface of concrete. Results are consistent with the analytical solution provided by Hagy and Gulati [20] and the previous experimental observations, confirming that the thicker the ice the greater the scaling damage.

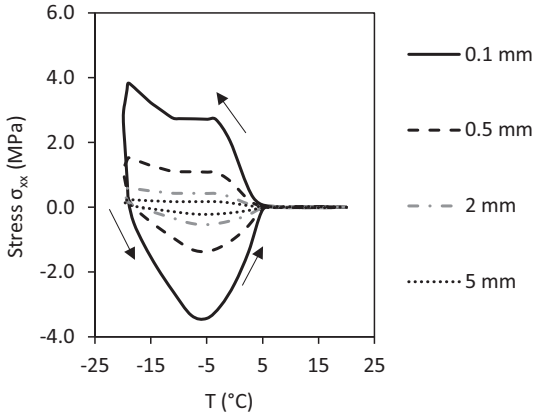

Fig. 9. Stress development at the gap between two-neighbouring ice-islands during a freeze thaw cycle for different gap sizes. The temperature was varied according to the cycle presented in Fig. 4. The arrows indicate the path of the temperature cycle.

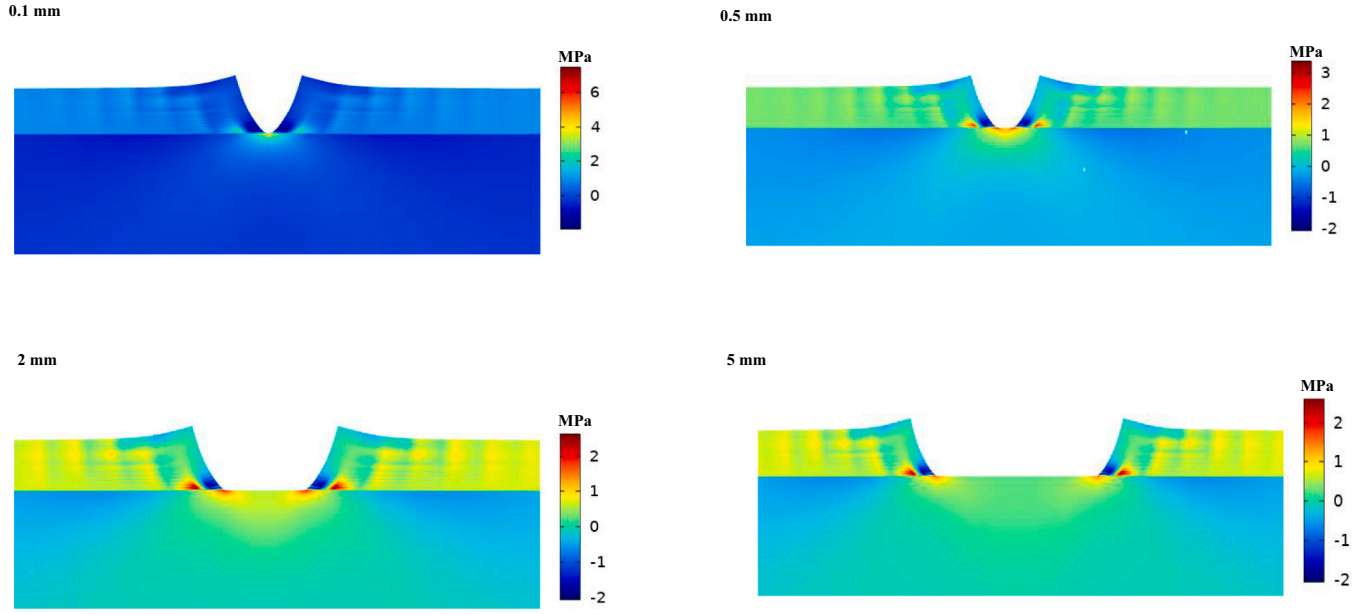

Fig. 10. Simulation of the effect of the gap size on the σ_{xx} stress distribution in the bi-layer material ice/concrete material. The two-ice-islands have a width of 25 mm and thickness of 2 mm. The gap between the neighbouring islands was varied from 0.1 mm up to 5 mm. Results corresponding to $t = 12$ h and T = −20 °C.

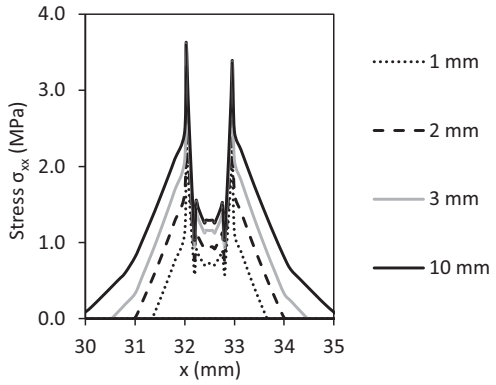

Fig. 11. Results of the simulation corresponding to the case 4 where the thicknesses of the two ice-islands covering the concrete was varied from 1 mm to 10 mm, while keeping the ice width at 25 mm and the gap size at 1 mm. The results corresponds to the uppermost surface of concrete (y = 20 mm), $t = 16$ h and T = −20 °C.

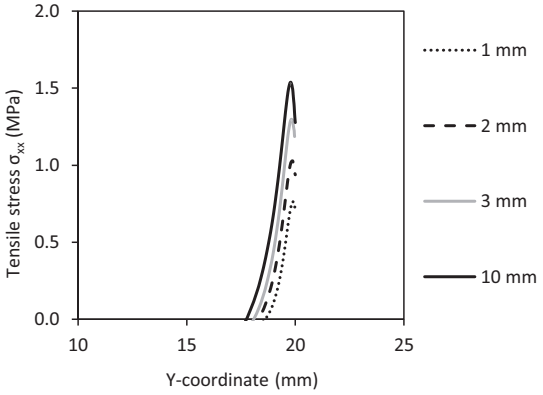

Fig. 12. Distribution of tensile stress σ_{xx} along the y-axis for the upper part of the concrete body that is prone to surface scaling.

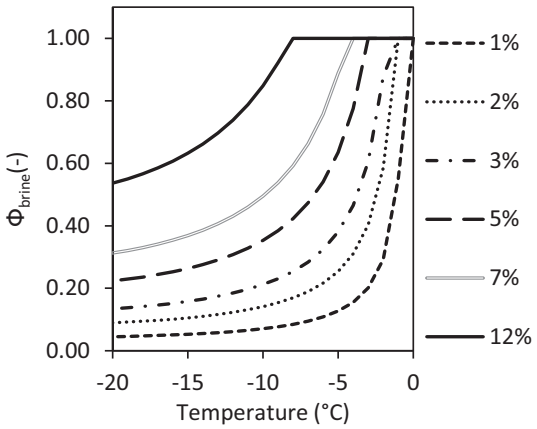

Fig. 13. Ice volume fraction (−) vs. temperature and salinity. Ice volume fractions are estimated based on NaCl-H2O phase diagram using the lever rule, where $\Phi_{ice} = 1 - W_0/W_T$; W_0 being the original concentration of the solution and W_T is the liquidus concentration at temperature T. An illustration of the lever rule can be found in [7]. The corresponding brine fraction can be estimated using the equation $\Phi_{brine} = 1 - \Phi_{ice}$.

In Fig. 12 the stresses parallel to the x-axis (σ_{xx}) at the center of the gap between the two neighbouring-ice-islands along the y-axis are presented for different ice thicknesses at t = 12 h and T = −20 °C. For convenience, only the positive stresses (i.e. tension) in the upper surface of concrete (y > 10 mm) are presented. It can be seen that the area under the curve where the stress $\sigma_{xx} > 0$ is increasing with increasing ice thickness. This together with the increasing stress with increasing ice thickness noted earlier (Fig. 11) suggest that the damaged zone is greater for the thicker ice. It can be also noted that the depth of the damage zone increases as the thickness of the ice increases.

4. Discussion

When a bi-layer structure composed of film covering a substrate is subjected to cooling, the large mismatch between the coefficients of thermal expansion and the Young's modulus of the film and the substrate

creates a state of tensile stress in the film (=ice) and compressive stress state at the substrate region (=concrete) near the film, when the film has a larger thermal coefficient [28,29]. In the case of a continuous ice layer fully covering the surface of concrete (as in Fig. 3.a), the ice having a higher thermal expansion coefficient, will develop tensile stresses upon cooling. While the upper surface of concrete in contact with ice will be in a compressive stress state, as it was demonstrated in Fig. 5. Consequently, no failure under tensile stress is expected. The analysis presented here confirms that the presence of gaps between neighbouring ice-islands is crucial for the build-up of tensile stresses at the concrete surface, which is in line with the experimental observations by Valenza and Scherer [7]. Furthermore, it is demonstrated that the gap size between two ice-islands and their distribution change the magnitude of scaling during freeze-thawing of concrete: the narrower the gap (i.e. the thinner the crack or the smaller the defect) the higher the tensile (glue-spall) stress.

In the following an explanation of FSS is provided based on the dynamics of saline-ice upon freezing. For instance, using the NaCl-H_2O phase diagram, the fraction of the ice is calculated and presented for different salinities and temperatures in Fig. 13. As it can be seen from Fig. 13, for the range of temperatures usually considered in frost testing (up to −20 °C), the brine volume fraction at a given temperature is increasing with increasing salt concentration. For example, the brine volume fraction increases from 0% in a pure ice, to occupying 53% of the 12% NaCl-Ice. During freeze-thawing of pure water (0%) on concrete there will be no brine pockets on the surface of concrete. Instead, a homogenous ice layer will fully cover the surface of concrete. The absence of gaps during freeze-thawing of concrete reduces the scaling likelihood, as shown in Fig. 5. This strengthens the idea that upon freeze-thawing of concrete exposed to pure water, no scaling will occur as pure ice does not have brine channels/brine pockets, which is consistent with experimental observations [11,17].

Instead, when freezing a saline solution on concrete, various ice-islands will cover the surface, leaving brine channels filled with liquid. Based on the simulation presented in Fig. 5, the FSS damage is dependent on the presence of those brine channels and will be observed at the level of the brine channels/pockets depending on the tensile strength distribution at the concrete surface. These results compare well with experimental observations of Valenza and Scherer [6,12]. For instance, Valenza and Scherer [6,12] demonstrated that upon freezing an isolated ice cube on a mortar surface, cracking at the surface is clearly visible at the perimeter of the ice-island during post-experiment inspection. The cracking of the concrete occurred although the pure ice itself did not crack, illustrating that the crack propagation in concrete based on ice fracture is not the only mechanism involved in FSS damage.

As for the ice microstructure, it was shown that both the ice-island width and distribution have a crucial role in the level of stress generated at the surface of concrete. For instance, increasing the island width increases the stress at the concrete surface. The same goes for the effect of reducing the gap size between two neighbouring-islands. The size of the gap has a more determinant effect compared to the island width. A gap of 0.1 mm between the two ice-islands, generated stresses as high as 3.7 MPa, which is above the average tensile strength of cement paste of around 3 MPa. The brine pores cover a wide range of sizes from few mm to few μm. The smallest pores, referred to as brine-layers have sizes in the sub-millimetre range and a spacing of around 1 mm [24]. A brine layer may disappear, join another brine layer or split into many layers upon ice growth [37,38]. A mathematical model developed by Lieblappen et al. [38] supported by X-ray micro-computed tomography imaging of sea-ice, have demonstrated that brine layers with size between 100 and 200 μm have a higher probability to remain during sea-ice growth. A brine channel of 100 μm in size that can generate tensile stress of 3.7 MPa (see Fig. 8) seems to form the majority of the brine. This suggests that FSS with NaCl concentration close to sea-ice concentration can generate tensile stresses capable of damaging cementitious materials. It is worth recalling that this stress estimated in this study corresponds to the 2D simulation and that even higher stresses might result from the interference of more than two islands in an FSS experiment. The experiments performed by Valenza and Scherer [7] to prove the significance of an ice-island in the build-up of stress, did not investigate the effect of the gap size between islands nor their width on the level of stress. These parameters are significant for the level of damage that is going to be observed during frost salt scaling. However, to the authors' knowledge, there are no experiments which can support the present simulations.

When the concentration of the saline solutions varies, the way ice is distributed on the concrete surface will be a result of its microstructure. The pessimum effect could for instance be qualitatively explained based on the glue-spall theory and the changing ice microstructure with salt concentration. For instance, two major changes occur when we freeze saline solutions with different concentrations. As seen in Fig. 13, at a given temperature, the brine fraction of the brine-ice composite solution increases with increasing salt concentration. At the same time, the size of the brine-pockets/channels varies with the brine fraction [39], and therefore will be different for different salt concentrations, at a given temperature. The literature regarding the changes of the sea-ice microstructure with the temperature is abundant [23,38–40]. However, very few studies (i.e. [41]) describe the evolution of the ice microstructure for different salt concentration and types of de-icers. Nevertheless, one could assume that the volume fraction of the ice (respectively brine) is the determinant parameter for the resultant ice microstructure, at given freezing rate and freezing conditions. Therefore, it is possible to make correlations between the freezing temperature and the salt concentration, at a similar ice/brine volume fraction. For instance, freezing a moderately concentrated saline solution at a certain temperature would generate the same brine fraction as freezing highly concentrated saline solution at a lower temperature. Such as a 12%-NaCl-ice will have a brine fraction of 53% at T = −20 °C, while a 2%-NaCl reaches the same value at T = −4 °C (Fig. 13). Hence, the ice microstructure generated upon increasing the temperature when freezing a saline solution at a given concentration, would be comparable to the one obtained upon increasing the salt concentration at a given temperature. Experimental investigation of sea ice with μ-computed tomography [39] showed that the brine channel size decreases as the fraction of the brine decreases when the temperature is decreased. Correspondingly, when freezing saline solutions with different concentrations down to the same temperature, the brine channel sizes will increase as the salt concentration increases. It was clear from Fig. 8 that the size of the gap (in our case brine channel) between two-neighbouring islands determines the magnitude of tensile stress that builds-up at the concrete surface, where decreasing the gap size leads to an increase in the stress magnitude at the level of the brine channel. Consequently, the increasing sizes of the brine channels upon increasing salt concentration will reduce the level of stresses at the brine channel. This would suggest that the scaling will decrease with increasing the concentration of the saline solution, which is not what is exactly seen during experiments, as the maximum damage occurs for moderately concentrated solutions. It is worth re-calling that the size of scaled particle covers the gap size and a small region nearby. This suggests an inter-dependence between the size of the scaled particle and the brine channel size. For instance, the smaller the brine channel the smaller the size of the scaled particle will be. Therefore, even if the small brine channel size results in high tensile stresses and higher probability of scaling, the scaled zone will be small. Also, the width of the ice-island will change with the salt concentration. It is clear that both the size of brine channels and the width of ice-island influence the amount of scaled material at each brine channel and the stress level. It is their combined effect which contributes to the pessimum effect. However, experimental input is needed for a more quantitative evaluation of the frost salt scaling magnitude. For instance, experimental quantification of the saline-ice microstructure at different salt concentration and types of de-icer is required to model the pessimum effect.

Another important observation during FSS is that increasing the thickness of ice, results in increasing scaling damage [15,16,42]. As seen in Fig. 11 the effect of the ice thickness layer on the FSS damage is quite direct from the simulation, and simply a thicker ice, results in higher tensile stress at the level of brine channels located at the concrete interface. Furthermore, recent analysis [7] based on fracture mechanics of thin film on a substrate, linked the likelihood of crack development in the concrete to the ice thickness. It was concluded from these analyses that increasing thickness of the ice layer, intensifies the concrete scaling as it results in higher crack depth and higher stress intensity factor at a given crack depth. These findings are coherent with results in Fig. 12 showing that the depth of the damaged zone increased as the thickness of the ice increased. In the different standards available for FSS testing, the thickness of the ice layer varies between 3 and 10 mm. The ice thickness is a determinant parameter in the level of scaling and hence results of the different testing standards would not be easily comparable.

The visco-elastic analysis of stresses in the ice by Valenza and Scherer [7] correlated the pessimum effect to the increasing ability of ice to crack as the salt concentration increases and that cracking of ice will lead to propagating of assumed pre-existing cracks in the concrete. Now similarly to the glue-spalling process where the glass is sand-blasted to create flaws, the uppermost surface of concrete might contain initial flaws and cracks which might propagate further as a result of ice cracking. However, it is demonstrated in the present study that independently of the presence of initial flaws, the surface of concrete might scale as a result of the presence of individual ice-islands separated by brine channels (gaps). In the analysis by Valenza and Scherer [7], the brine concentration controls the ice cracking. Here it suggested that the changing microstructure of the brine-ice composite with salt concentration and temperature is responsible for the pessimum effect. Furthermore, the simulations in Fig. 11 show that the glue-spall when considering heterogenous ice explains the effect of increasing ice layer thickness on the scaling increase, which could not be explained based on the ice fracture behaviour.

The analysis presented here is a direct application and extension of the glue-spall theory that account for the different observations related to frost salt scaling. However, the concrete was treated as a homogenous non-porous material. In particular, concrete specimens without air pores, expand upon freezing if the pore system is highly saturated, while sufficiently air-entrained concretes show a net contraction [33]. The simulation in this study does not account for this expansion observed for non-air entrained concrete, and the simulated tensile stresses will be even higher if this expansion is considered. A more complete study of the FSS mechanisms would require considering the hygro-thermo-mechanical response of concrete during freeze-thawing combined with the glue-spall theory. This will help to better understand the mechanisms involved in frost salt scaling and define the parameters to better control the concrete performance against frost salt testing.

5. Conclusion

The glue-spall mechanism suggested responsible for frost salt scaling of concrete exposed to salt solutions is presented, modelled, and discussed. It was demonstrated that the presence of brine channels between ice-islands on the concrete surface is a prerequisite for the scaling during freeze-thawing of concrete in the presence of salt. Observations of the effect of salt concentration and the thickness of the brine-ice layer on frost-salt scaling were explained assuming concentration and temperature dependent geometry of ice and brine. For instance, pure water does not cause scaling simply because there are no brine pockets in pure ice, which contributes to less stress. Furthermore, the increasing scaling for increasing ice thickness and the existence of a pessimum concentration were explained through modelling. The ice microstructure seems to play a determinant role on the level of frost salt scaling. The pessimum effect appears to be the result of the fraction of the brine determining the size of ice-island on the concrete surface and the size of the brine channels (gaps) between them.

CRediT authorship contribution statement

Sara Bahafid: Conceptualization, Methodology, Validation, Investigation, Data curation, Writing - original draft, Writing - review & editing, Visualization, Project administration.

Max Hendriks: Conceptualization, Methodology, Writing - review & editing, supervision.

Stefan Jacobsen: Conceptualization, Methodology, Writing - review & editing.

Mette Geiker: Conceptualization, Methodology, Writing - review & editing, Supervision, Funding acquisition.

Declaration of competing interest

All authors certify that they have NO affiliations with or involvement in any organization or entity with any financial interest (such as honoraria; educational grants; participation in speakers' bureaus; membership, employment, consultancies, stock ownership, or other equity interest; and expert testimony or patent-licensing arrangements), or non-financial interest (such as personal or professional relationships, affiliations, knowledge or beliefs) in the subject matter or materials discussed in this manuscript.

Acknowledgements

This research was funded by Nanocem, the industrial-academic nanoscience research network for sustainable cement and concrete (www.nanocem.org). Discussion with Sønke Maus, NTNU, on the microstructure of frozen saline solutions (brine-ice composites) is highly appreciated.

References

[1] J. Kaufmann, Experimental identification of damage mechanisms in cementitious porous materials on phase transition of pore solution under frost deicing salt attack. 2000. Thèse de doctorat. Swiss Federal Institut of Technology Lausanne (EPFL).
[2] M. Wu, K. Fridh, B. Johannesson, M. Geiker, Influence of frost damage and sample preconditioning on the porosity characterization of cement based materials using low temperature calorimetry, Thermochim. Acta 607 (May 2015) 30–38.
[3] T.C. Powers, Structure and physical properties of hardened Portland cement paste, Am. Ceram. Soc. 41 (1) (1958) 6.
[4] T.C. Powers, Freezing effects in concrete, Durab. Concr. 47 (Jan. 1975) 1–11.
[5] W. Studer, Internal comparative tests on frost deicing salt resistance, in: Rılem Proceedıngs 30Freeze-Thaw Durability of Concrete, 2020, pp. 269–280.
[6] F. Gong, S. Jacobsen, Modeling of water transport in highly saturated concrete with wet surface during freeze/thaw, Cem. Concr. Res. 115 (Jan. 2019) 294–307.
[7] J.J. Valenza, G.W. Scherer, Mechanism for salt scaling, J. Am. Ceram. Soc. 89 (4) (2006) 1161–1179.
[8] Z. Sun, G.W. Scherer, Effect of air voids on salt scaling and internal freezing, Cem. Concr. Res. 40 (2) (2010) 260–270.
[9] G. Fagerlund, Frost resistnace of high performance concrete–some theoritical considerations: a contribution to RILEM-3C-Workshop 'Durability of high performance concrete, in: Wien 14th-15th February, February (Report TVBM; Vol 3056), Division of Building Materials, Lund University, 1994.
[10] S. Jacobsen, D.H. Sœther, E.J. Sellevold, Frost testing of high strength concrete: frost/salt scaling at different cooling rates, Mater. Struct. Constr. 30 (1) (1997) 33–42.
[11] G.J. Verbeck, P. Klieger, Studies of 'Salt' scaling of concrete, Highw. Res. Board Bull. 150 (1957) 1–13.
[12] J.J. Valenza, G.W. Scherer, A review of salt scaling: I. Phenomenology, Pergamon, Cement and Concrete Research 37 (7) (2007) 1007–1021, 01-Jul.
[13] J.J. Valenza, G.W. Scherer, A review of salt scaling: II. Mechanisms, Elsevier Ltd, Cement and Concrete Research 37 (7) (2007) 1022–1034, 01-Jul.
[14] A.Harry Arnfelt, Damage on Concrete Pavements by Wintertime Salt Treatment, Medd. 66 Statens Väginstitut, 1943.
[15] O. Çopuroğlu, E. Schlangen, Modeling of frost salt scaling, Cem. Concr. Res. 38 (1) (2008) 27–39.
[16] M.-H. Tremblay, F. Lory, J. Marchand, G.W. Scherer, J.J. Valenza, Ability of the glue spall model to account for the de-icer salt scaling deterioration of concrete, in: 12th International Congress on the Chemistry of Cement, 2007, pp. 1–12.
[17] P. Klieger, Durability studies at the portland cement association, in: Durability of Building Materials and Components, 2009, 282-282–19.

[18] G. Fagerlund, M. Setzer, Freeze-thaw and de-icing resistance of concrete, in: RILEM Committee TC-117 FDC, Lund Institute of Technology Research Seminar Held in Lund, 1991, pp. 1–165.
[19] J.J. Valenza, G.W. Scherer, Mechanism for salt scaling of a cementitious surface, Mater. Struct. Constr. 40 (3) (2007) 259–268.
[20] S.T. Gulati, H.E. Hagy, Analysis and measurement of glue-spall stresses in glass-epoxy bonds, J. Am. Ceram. Soc. 65 (1) (1982) 1–5.
[21] K.D. Vaudrey, Ice engineering: Study of Related Properties of Floating Sea-ice Sheets and Summary of Elastic and Viscoelastic Analyses, 1977.
[22] G.W. Timco, S. O'Brien, Flexural strength equation for sea ice, Cold Reg. Sci. Technol. 22 (3) (Mar. 1994) 285–298.
[23] K. Morawetz, S. Thoms, B. Kutschan, Formation of brine channels in sea ice, Eur. Phys. J. E 40 (3) (2017).
[24] F. Cottier, P. Wadhams, Linkages between salinity and brine channel distribution in young sea ice, J. Geophys. Res. 104 (1999) 859–871.
[25] S. Maus, M. Schneebeli, A. Wiegmann, An X-ray micro-tomographic study of the pore space, permeability and percolation threshold of young sea ice, Cryosph. Discuss. (2020) 1–30.
[26] M. Nakawo, N.K. Sinha, A note on brine layer spacing of first-year sea ice, Atmos. - Ocean 22 (2) (1984) 193–206.
[27] P. Barnes, D. Tabor, J.C.F. Walker, The friction and creep of polycrystalline ice, Proceedings of the Royal Society of London, A. Mathematical and Physical Sciences 324 (1557) (1971) 127–155. http://www.jstor.
[28] M.F. Ashby, P. Duval, The creep of polycrystalline ice, Cold Reg. Sci. Technol. 11 (3) (Nov. 1985) 285–300.
[29] R. Duddu, H. Waisman, A temperature dependent creep damage model for polycrystalline ice, Mech. Mater. 46 (Mar. 2012) 23–41.
[30] D.G. Karr, K. Choi, A three-dimensional constitutive damage model for polycrystalline ice, Mech. Mater. 8 (1) (1989) 55–66.
[31] I. Maruyama, H. Sasano, Y. Nishioka, G. Igarashi, Strength and Young's modulus change in concrete due to long-term drying and heating up to 90°C, Cem. Concr. Res. 66 (2014) 48–63.
[32] T. Gasch & A. Ansell, Cracking in quasi-brittle materials using isotropic damage mechanics. In Comsol Conference Proceedings (2016).
[33] D. Eriksson, T. Gasch, R. Malm, A. Ansell, Freezing of partially saturated air-entrained concrete: a multiphase description of the hygro-thermo-mechanical behaviour, Int. J. Solids Struct. 152–153 (2018) 294–304.
[34] J. Rumble, CRC Handbook of Chemistry and Physics, in: CRC Handbook of Chemistry & Physics, 1997.
[35] K.H. Kim, S.E. Jeon, J.K. Kim, S. Yang, An experimental study on thermal conductivity of concrete, Cem. Concr. Res. 33 (3) (Mar. 2003) 363–371.
[36] T. Gasch, Concrete as a multi-physical material with applications to hydro power facilities, in: KTH Royal Institute of Technology, 2016.
[37] R.M. Lieb-Lappen, E.J. Golden, R.W. Obbard, Metrics for interpreting the microstructure of sea ice using X-ray micro-computed tomography, Cold Reg. Sci. Technol. 138 (Jun. 2017) 24–35.
[38] R.M. Lieblappen, D.D. Kumar, S.D. Pauls, R.W. Obbard, A network model for characterizing brine channels in sea ice, Cryosphere 12 (3) (2018) 1013–1026.
[39] D.J. Pringle, J.E. Miner, H. Eicken, K.M. Golden, Pore space percolation in sea ice single crystals, J. Geophys. Res. Ocean. 114 (12) (2009) 1–14.
[40] W.F. Weeks, Tensile strength of NaCl ice, J. Glaciol. 4 (31) (1962) 25–52.
[41] Ľ. Vetráková, V. Neděla, J. Runštuk, D. Heger, The morphology of ice and liquid brine in the environmental SEM: a study of the freezing methods, Cryosph. Discuss. (2019) 1–28.
[42] M. Müller, H. Ludwig, Salt frost scaling of concrete—effect of glue spalling. In: Paper presented at the concrete 2017 conference, Adelaide, Australia, October 22–25, 2017.